Advances in Applied Mathematics and Mechanics
Adv. Appl. Math. Mech., Vol. **4**, No. 6, pp. 799-820

DOI: 10.4208/aamm.12-12S10
December 2012

Modification of Multiple Knot B-Spline Wavelet for Solving (Partially) Dirichlet Boundary Value Problem

Fatemeh Pourakbari and Ali Tavakoli*

Department of Mathematics, Vali-e-Asr University of Rafsanjan, Iran

Received 15 December 2011; Accepted (in revised version) 16 July 2012

Available online 9 November 2012

Abstract. A construction of multiple knot B-spline wavelets has been given in [C. K. Chui and E. Quak, Wavelet on a bounded interval, In: D. Braess and L. L. Schumaker, editors. Numerical methods of approximation theory. Basel: Birkhauser Verlag; (1992), pp. 57–76]. In this work, we first modify these wavelets to solve the elliptic (partially) Dirichlet boundary value problems by Galerkin and Petrov Galerkin methods. We generalize this construction to two dimensional case by Tensor product space. In addition, the solution of the system discretized by Galerkin method with modified multiple knot B-spline wavelets is discussed. We also consider a nonlinear partial differential equation for unsteady flows in an open channel called Saint-Venant. Since the solving of this problem by some methods such as finite difference and finite element produce unsuitable approximations specially in the ends of channel, it is solved by multiple knot B-spline wavelet method that yields a very well approximation. Finally, some numerical examples are given to support our theoretical results.

AMS subject classifications: 65T60, 35L60, 35L04

Key words: Galerkin method, semi-orthogonal, B-spline wavelet, multi-resolution analysis, tensor product, hyperbolic partial differential equation, Saint-Venant equations.

1 Introduction

Solving boundary value problems by Galerkin methods leads to very large systems $Ax = b$. Then, for numerical implementation, it is necessary to generate a sparse matrix A. In order to do this, the basis functions with local support are suitable. In particular, orthonormal basis functions with local support decrease the expenses of numerical implementation. However, construction of orthonormal basis functions

*Corresponding author.
URL: `http://tavakoli@vru.ac.ir`
Email: f.pourakbari@stu.vru.ac.ir (F. Pourakbari), tavakoli@mail.vru.ac.ir (A. Tavakoli)

with local support is not easy. Although, Daubechies et al. in [12] have given such basis functions in wavelet space, but there is no still explicit formulas. Then, the scientists have tried to construct semi-orthogonal basis wavelets with local support and explicit formulas. This can be done by multiple knot B-splines (see [9] and [7]). In this work, by multiple knot B-spline functions, we construct the wavelets that satisfy in the (partially) Dirichlet boundary conditions.

Let us first recall the notions of scaling function and multi-resolution analysis as introduced in [16] and [18]. For a function $\phi \in L^2(\Omega)$, let a reference subspace V_0 be generated as the L^2-closure of the linear span of the integer translates of ϕ, namely:

$$V_0 := clos_{L^2}\langle \phi(. - k) : k \in \mathcal{I}_0 \rangle$$

and consider the other subspaces $V_j := clos_{L^2}\langle \phi_{j,k} : k \in \mathcal{I}_j \rangle, j \geq 0$, where $\phi_{j,k} := 2^{j/2}\phi(2^j . - k), j \geq 0, k \in \mathcal{I}_j$, where $\langle F \rangle$ and $\mathcal{I}_j$ denote the space spanned by F and some appropriate set of indices, respectively.

Definition 1.1. *A function $\phi \in L^2(\Omega)$ is said to generate a multi-resolution analysis (MRA) if it generates a nested sequence of closed subspace V_j that satisfy*

(i) $V_0 \subset V_1 \subset \cdots;$

(ii) $clos_{L^2}(\cup_{j \geq 0} V_j) = L^2(\Omega);$

(iii) $\cap_{j \in \mathbb{Z}} V_j = \{0\};$

(iv) $f \in V_j \Longleftrightarrow f(. + 2^{-j}) \in V_j \Longleftrightarrow f(2.) \in V_{j+1},\ j \geq 0;$

(v) $\{\phi_{j,k}\}_{k \in \mathcal{I}_j}$ forms a Riesz basis for V_j, i.e.,

there are constants A and B with $0 < A \leq B < \infty$ such that

$$A \sum_{k \in \mathcal{I}_j} |c_k|^2 \leq \| \sum_{k \in \mathcal{I}_j} c_k \phi_{j,k} \|^2_{L^2(\Omega)} \leq B \sum_{k \in \mathcal{I}_j} |c_k|^2$$

independent of j.

If ϕ generates an MRA, then ϕ is called a scaling function. In case different integer translates of ϕ are orthogonal ($\phi(. - k) \perp \phi(. - \tilde{k})$, for $k \neq \tilde{k}$), the scaling function is called an orthogonal scaling function.

Since the subspace V_j are nested, there exists a subspace W_j, such that

$$V_{j+1} = V_j \oplus W_j, \qquad j \in \mathbb{Z},$$

where W_j is some direct summand, not necessarily the orthogonal one. Then, the problem of constructing the spaces W_j means to find a stable system of functions $\Psi_j =$

$\{\psi_{j,k}:\ k\in\Gamma_j\}$, such that $W_j=clos_{L^2}\langle\psi_{j,k}:k\in\Gamma_j\rangle$, $j\geq 0$, where $\psi_{j,k}:=2^{j/2}\psi(2^j.-k)$, $k\in\Gamma_j\rangle$, $j\geq 0$. For abbreviation, we set $W_{-1}=V_0$, $\Gamma_{-1}=\mathcal{I}_0$ and hence this gives rise to a decomposition of V_j, namely

$$V_j=\bigoplus_{k=-1}^{j-1}W_k.$$

Definition 1.2. *The elements of* Ψ_j *are called a set of wavelets, if the system* $\Psi=\bigcup_{j=-1}^{\infty}\Psi_j$ *forms a Riesz basis for* $L^2(\Omega)$*, i.e.,*

$$\|\sum_{j\geq -1}\sum_{k\in\Gamma_j}d_{j,k}\Psi_{j,k}\|^2_{L^2(\Omega)}\sim\sum_{j\geq -1}\sum_{k\in\Gamma_j}|d_{j,k}|^2.$$

If $(\psi_{j,k},\psi_{j,m})=\delta_{k,m}$, $k,m\in\Gamma_j$, *where* $(f,g)=\int_\Omega f(x)\overline{g(x)}dx$ *is the standard inner product, then* ψ *is called an orthonormal wavelet. The wavelets* $\psi_{j,k}$ *are called semi-orthogonal, if* $(\psi_{j,k},\psi_{\tilde{j},\tilde{k}})=0$; $j\neq\tilde{j}$ *for all* $j,\tilde{j}\geq -1$, $k\in\Gamma_j,\tilde{k}\in\Gamma_{\tilde{j}}$.

We denote the multi-resolution space V_j and the wavelet space W_j on bounded interval $[0,1]$ by $V_j^{[0,1]}$ and $W_j^{[0,1]}$ for any $j\geq 0$, respectively.

2 Multiple knot B-spline wavelets for $L^2[0,1]$

In this section, we give the semi-orthogonal spline wavelets in $L^2[0,1]$ that has been constructed by Chui and Quak (see [9]). We have modified some proofs in [9] that were not clear. Let $m\in\mathbb{N}$ be fixed throughout this section.

Definition 2.1. *For* $j\in\mathbb{Z}_+$, *let a knot sequence on* $[0,1]$ *be given by* $\mathbf{t}^{(j)}:=\mathbf{t}_m^{(j)}:=\{t_k^{(j)}\}_{k=-m+1}^{2^j+m-1}$ *with*

$$t^{(j)}_{-m+1}=t^{(j)}_{-m+2}=\cdots=t^{(j)}_0=0,\tag{2.1a}$$
$$t^{(j)}_k=k2^{-j},\quad (k=1,\cdots,2^j-1),\tag{2.1b}$$
$$t^{(j)}_{2^j}=t^{(j)}_{2^j+1}=\cdots=t^{(j)}_{2^j+m-1}=1.\tag{2.1c}$$

The (polynomial) spline space of order m for the knot sequence $\mathbf{t}_m^{(j)}$ is defined as

$$S_{m,j}:=S_{m,\mathbf{t}_m^{(j)}}:=\big\{s\in C^{m-2}[0,1]:s|(t_k^{(j)},t_{k+1}^{(j)})\in\Pi_{m-1},\ k=0,\cdots,2^j-1\big\}.$$

The sequence of subspaces $V_j^{[0,1]}$ is given by

$$V_j^{[0,1]}:=S_{m,j},\quad V_0^{[0,1]}:=\Pi_{m-1}.\tag{2.2}$$

By standard spline theory one can establish the following:

Theorem 2.1. *A basis for* $V_j^{[0,1]}$ *is given by the B-spline* $B_{i,m,j}$, $i = -m+1,\cdots,2^j-1$ *and thus*

$$dimV_j^{[0,1]} = 2^j + m - 1.$$

Here,

$$B_{i,m,j}(x) := (t^j_{i+m} - t^j_i)[t^j_i, t^j_{i+1},\cdots,t^j_{i+m}]_t(t-x)_+^{m-1},$$

where $[\cdot,\cdots,\cdot]_t$ is the mth divided difference of $(t-x)_+^{m-1}$ with respect to the variable t. The support of $B_{i,m,j}$ is $[t_i^{(j)}, t_{i+m}^{(j)}]$. For $i = -m+1,\cdots,-1$, the knot sequence defining $B_{i,m,j}$ contains a multiple knot at 0, and for $i = 2^j - m + 1,\cdots,2^j-1$, a multiple knot at 1. The inner ones ($i = 0,\cdots,2^j - m$ for $2^j \geq m$) are just dilation and translation of the cardinal B-spline $N_m(x) = m[0,1,\cdots,m]_t(t-x)_+^{m-1}$ used as the scaling function for $L^2(\mathbb{R})$, namely:

$$B_{i,m,j} = N_m(2^j.-i), \quad i = 0,\cdots,2^j - m.$$

To find suitable wavelet function spanning $W_j^{[0,1]}$ in the orthogonal decomposition $V_{j+1}^{[0,1]} = V_j^{[0,1]} \oplus W_j^{[0,1]}$, we use an argument that identifies the wavelet space $W_j^{[0,1]}$ with a subspace of a spline of order $2m$. For each $m \in \mathbb{N}$, define the spline space

$$\tilde{S}_{2m,\mathbf{t}_{2m}^{(j+1)}} := \langle B_{i,2m,\mathbf{t}_{2m}^{(j+1)}} : \ i = -m+1,\cdots,2^{j+1}-m-1\rangle$$

and its subspace

$$\tilde{S}^0_{2m,\mathbf{t}_{2m}^{(j+1)}} := \big\{ s \in \tilde{S}_{2m,\mathbf{t}_{2m}^{(j+1)}} : \ s(t_k^{(j)}) = 0, \ \ k = 0,\cdots,2^j \big\}$$

of all splines in $\tilde{S}_{2m,\mathbf{t}_{2m}^{(j+1)}}$ that vanish on the coarse knot sequence $\mathbf{t}_{2m}^{(j)}$. The following theorem states that for constructing a wavelet basis in $W_j^{[0,1]}$, we only need to form a basis in $\tilde{S}^0_{2m,\mathbf{t}_{2m}^{(j+1)}}$:

Theorem 2.2. *For each* $m \in \mathbb{N}$, *the* m*-th order differential operator* D^m *maps the space* $\tilde{S}^0_{2m,\mathbf{t}_{2m}^{(j+1)}}$ *one-to-one onto the wavelet space* $W_j^{[0,1]}$.

Proof. See [9]. □

In chui-Wang [10], an interpolatory wavelet on $\mathbb{R}$ is defined as the m-th derivative of the fundamental cardinal spline $L_{2m}(k) = \delta_{0,k}$, $k \in \mathbb{Z}$. Analogously, $W_j^{[0,1]}$ is spanned by the m-th derivatives of the fundamental splines $L_{i,2m}$ in $\tilde{S}^0_{2m,\mathbf{t}_{2m}^{(j+1)}}$, for which $L_{i,2m}((2k-1)2^{-j-1}) = \delta_{i,k}$, $i,k = 1,\cdots,2^j$.

Theorem 2.3. *The wavelet space* $W_j^{[0,1]}$ *is spanned by function* $\psi^I_{i,m} = L^{(m)}_{i,2m}$, $i = 1, \cdots, 2^j$, *where for* $k = 1, \cdots, 2^{j+1} - 1$, $L_{i,2m} \in \tilde{S}^0_{2m,\mathbf{t}^{(j+1)}_{2m}}$ *satisfy*

$$L_{i,2m}(t_k^{(j+1)}) = \begin{cases} 1, & \text{for } k = 2i-1, \\ 0, & \text{otherwise}. \end{cases} \tag{2.3}$$

Let $\mathcal{B}$ *be the* $(2^{j+1} - 1) \times (2^{j+1} - 1)$ *so-called collocation matrix with entries* $b_{k,\tilde{i}} = B_{\tilde{i}-m,2m,\mathbf{t}^{(j+1)}_{2m}}(t_k^{(j+1)})$, *for* $\tilde{i}$, $k = 1, \cdots, 2^{j+1} - 1$, *and let* $B_{k,\ell}$ *be its minor that are obtained by deleting the* k*-th row and* ℓ*-th column. Then, the* $L_{i,2m}s'$ *can be compute*

$$L_{i,2m}(x) = \sum_{\ell=1}^{2^{j+1}-1} (-1)^{2i-1+\ell} B_{2i-1,\ell} B_{\ell-m,2m,\mathbf{t}^{(j+1)}_{2m}}(x) \Big/ det\mathcal{B}. \tag{2.4}$$

Proof. Since the splines $B_{\tilde{i}-m,2m,\mathbf{t}^{(j+1)}_{2m}}$ for $\tilde{i} = 1, \cdots, 2^{j+1} - 1$, are linearly independent and entries on diagonal of $\mathcal{B}$ are nonzero, then $det\mathcal{B}$ is nonzero. As a function of x, suppressing the second and third indices of the B-spline, we see that the expression

$$det \begin{bmatrix} B_{-m+1}(t_1^{(j+1)}) & \cdots & B_{2^{j+1}-1-m}(t_1^{(j+1)}) \\ \vdots & \vdots & \vdots \\ B_{-m+1}(x) & \cdots & B_{2^{j+1}-1-m}(x) \\ \vdots & \vdots & \vdots \\ B_{-m+1}(t^{(j+1)}_{2^{j+1}-1}) & \cdots & B_{2^{j+1}-1-m}(t^{(j+1)}_{2^{j+1}-1}) \end{bmatrix}, \quad (2i-1) - th\ row \tag{2.5}$$

vanishes at all knots except $t^{(j+1)}_{2i-1}$. For construction of $L_{i,2m}$, one can expand the determinant (2.5) with respect to the $(2i-1)$-th row and then normalizing appropriately gives (2.4). Now, let $\sum_{i=1}^{2^j} c_i L_{i,2m}(x) = 0$ for some c_i, $i = 1, \cdots, 2^j$. Then letting $x = t^{(j+1)}_{2i-1}$ and considering the relation (2.3), the coefficients c_i are zero that yield $L_{i,2m}$, for $i = 1, \cdots, 2^j$ are independent. Also, $L_{i,2m}(t_k^j) = 0$ for $k = 0, \cdots, 2^j$ and so are elements of $\tilde{S}^0_{2m,\mathbf{t}^{(j+1)}_{2m}}$ that consist a basis of this space. Hence, by Theorem (2.2), the m-th derivatives form a basis of $W_j^{[0,1]}$. □

Now, the following lemma ensures us that the interpolatory wavelets (2.4) are semi-orthogonal.

Lemma 2.1. *Let* $L^{(m)}_{i,2m}$, $i = 1, \cdots, 2^j$, *be the same interpolatory wavelets that given before. Then these wavelets are semi-orthogonal.*

Proof. It is suffices to show that $W_j^{[0,1]} \perp V_j^{[0,1]}$. By considering $L^{(\ell)}_{i,2m}(0) = L^{(\ell)}_{i,2m}(1) =$

0, for $\ell = 0, \cdots, m-1$ and integrating by parts $m-1$ times, we have:

$$\begin{aligned}\int_0^1 L_{i,2m}^{(m)}(x) B_{i,m,j}(x)dx &= \int_0^1 (-1)^{m-1} L'_{i,2m}(x) B_{i,m,j}^{(m-1)}(x)dx \\ &= \sum_{k=0}^{2^j-1} \int_{t_k^{(j)}}^{t_{k+1}^{(j)}} (-1)^{m-1} L'_{i,2m}(x) B_{i,m,j}^{(m-1)}(x)dx \\ &= (-1)^{m-1} \sum_{k=1}^{2^j-1} \int_{t_k^{(j)}}^{t_{k+1}^{(j)}} L'_{i,2m}(x) c_k dx \\ &= (-1)^{m-1} \sum_{k=1}^{2^j-1} c_k [L_{i,2m}(t_{k+1}^{(j)}) - L_{i,2m}(t_k^j)] \\ &= 0.\end{aligned}$$

In the above equalities, we have used this fact that $B_{i,m,j}^{(m-1)} \equiv c_k$ on $(t_k^{(j)}, t_{k+1}^{(j)})$ with c_k as a constant value and $L_{i,2m}$ vanishes at the original knots $t_k^{(j)}$ for $k = 0, \cdots, 2^j$. □

Unfortunately, the basis functions for $W_j^{[0,1]}$ in Theorem (2.3) have support on all of the interval $[0,1]$ and depend on all the functions $B_{i,2m,\mathbf{t}_{2m}^{(j+1)}}$ that numerically produce a long CPU time and fairly large errors. Chui and Wang in [9] have presented a basis of $W_j^{[0,1]}$ with localize supports and a clear distinction between boundary and inner wavelets. The following lemma describes the inner wavelets in $W_j^{[0,1]}$ with compact supports.

Lemma 2.2. *For all $j \in \mathbb{N}$ such that $2^j \geq 2m-1$, there exists $2^j - 2m + 2$ linearly independent inner wavelet $\psi_{j,i}$, $i = 0, \cdots, 2^j - 2m + 1$, in $W_j^{[0,1]}$ which are given by*

$$\psi_{j,i}(x) = \frac{1}{2^{2m-1}} \sum_{k=0}^{2m-2} (-1)^k N_{2m}(k+1) B^{(m)}_{2i+k,2m,\mathbf{t}_{2m}^{(j+1)}}(x).$$

Proof. See [9]. □

By Lemma 2.2 there exist $2^j - 2m + 2$ inner wavelets and consequently $2m-2$ boundary wavelets need to be constructed. This task can be split into the construction of $m-1$ so-called 0-boundary wavelets, i.e., wavelets whose support contains the left endpoint of the interval $[0,1]$. By symmetry, the so-called 1-boundary wavelets are obtained from the 0-boundary wavelets by an index transformation $i \longleftrightarrow 2^j - 2m + 1 - i$ and $x \longleftrightarrow 1 - x$. We have the following lemma for 0-boundary wavelets:

Lemma 2.3. *For $j \in \mathbb{Z}_+$, if $2^j \geq 2m-1$, there exist $m-1$ wavelets on the 0-boundary which* *can write as*

$$\begin{aligned}\psi_{j,i}(x) =&\frac{1}{2^{2m-1}}\sum_{k=-m+1}^{-1}\alpha_{i,-k}B^{(m)}_{k,2m,\mathbf{t}^{(j+1)}_{2m}}(x)\\&+\frac{1}{2^{2m-1}}\sum_{k=0}^{2m-2+2i}(-1)^kN_{2m}(k+1-2i)B^{(m)}_{k,2m,\mathbf{t}^{(j+1)}_{2m}}(x)\end{aligned} \tag{2.6}$$

with supports $[0,(2m-1+i)2^{-j}]$ *for* $i=-m+1,\cdots,-1$. *The coefficients* $\alpha_i := (\alpha_{i,k})^\top_{1\le k\le m-1}$ *are derived by solving the linear system*

$$B\alpha_i = \boldsymbol{r}_i^\top, \quad (i=-m+1,\cdots,-1)$$

with

$$B := \big(B_{-k,2m,\mathbf{t}^{(j+1)}_{2m}}(t^{(j)}_\ell)\big)_{1\le \ell,k\le m-1} \quad \text{and} \quad \boldsymbol{r}_i := (r_{i,\ell})_{1\le\ell\le m-1},$$

where

$$r_{i,\ell} = -\sum_{k=0}^{2m-2+2i}(-1)^kN_{2m}(k+1-2i)N_{2m}(2\ell-k), \quad \ell=1,\cdots,m-1.$$

Proof. See [9]. □

Remark 2.1. We note that the B-spline wavelets are semi-orthogonal because $W_j^{[0,1]} = \langle L^{(m)}_{i,2m}, i=1,\cdots,2^j\rangle = \langle \psi_{j,i}, i=-m+1,\cdots,2^j-m\rangle$.

3 Homogenous multiple knot B-spline wavelets

In this section, we construct the homogenous basis functions for Dirichlet elliptic boundary value problem in one and two dimensional case. We first explain that some of the B-spline and wavelet basis functions given in the Section 2 are not homogenous that should be modified. For convenience, we use V_j and W_j stead $V_j^{[0,1]}$ and $W_j^{[0,1]}$, respectively.

3.1 One dimensional B-spline wavelets

We know the smoothness decreases by $r-1$ at the point with r-tuple knot. By (2.2), the basis functions of V_j belong to $C^{m-2}[0,1]$. On the other hand, by considering the structure of B-spline functions, it is seen that only the basis $B_{-m+1,m,j}$ and $B_{2^j-1,m,j}$ have m-tuple knot in $x=0,1$, respectively. This implies that $B_{-m+1,m,j}$ and $B_{2^j-1,m,j}$ belong to $C^{m-2-(m-1)}(\mathbb{R})$, i.e.,

$$B_{-m+1,m,j}(0)\neq 0, \quad B_{2^j-1,m,j}(1)\neq 0.$$

Hence, theses two functions do not satisfy in Dirichlet boundary conditions. Moreover, by (2.6) in the formula of wavelet functions on the zero, there exists the function $B^{(m)}_{-m+1,2m,\mathbf{t}^{(j+1)}_{2m}} \in C^{m-2}[0,1]$ with m-tuple knot in zero boundary that implies

$$B^{(m)}_{-m+1,2m,\mathbf{t}^{(j+1)}_{2m}}(0) \neq 0.$$

Hence, the wavelet functions on the zero boundary do not satisfy in Dirichlet boundary conditions. By the reflective property of wavelet basis, this is true for the wavelets on the boundary of $x = 1$. If we need to use the basis functions of V_{j+1}, i.e.,

$$\{B_{i,m,j}\}_{-m+1\leq i\leq 2^j-1} \cup \{\psi_{j,i}\}_{-m+1\leq i\leq 2^j-m} \tag{3.1}$$

satisfying homogenous Dirichlet boundary conditions, we omit the multiple knot B-splines that are not zero on the boundaries. We note that as opposed to the scaling functions, we can not omit the wavelets that does not vanish on the boundaries. This can be seen by

$$|V_{j+1}| = |V_j| + |W_j| \Rightarrow 2^{j+1} + m - 1 = (2^j + m - 1) + |W_j|,$$

that yields the dimension of the space W_j must be 2^j. The notation $|\cdot|$ denotes the cardinal of the corresponding space. We modify the boundary wavelet bases. To this end, we state the following theorem.

Theorem 3.1. *For $2^j \geq 2m-1$, the wavelet basis $\psi^N_{j,i}$ at level j by*

$$\psi^N_{j,i} := \begin{cases} \psi_{j,i} - \alpha_{j,i}B_{-m+1,m,j}, & i = -m+1,\cdots,-1, \\ \psi_{j,i}, & i = 0,\cdots,2^j-2m+1, \\ \psi_{j,i} - \beta_{j,i}B_{2^j-1,m,j}, & i = 2^j-2m+2,\cdots,2^j-m, \end{cases}$$

satisfies in the homogenous Dirichlet boundary conditions where

$$\alpha_{j,i} := \frac{\psi_{j,i}(0)}{B_{-m+1,m,j}(0)}, \quad \beta_{j,i} := \frac{\psi_{j,i}(1)}{B_{2^j-1,m,j}(1)}.$$

Proof. We define the space W^N_j on the interval $[0,1]$ by

$$W^N_j = \langle \psi^N_{j,i},\ i = -m+1,\cdots,2^j-m \rangle.$$

Let $I_j := \{-m+1,\cdots,2^j-1\}$ and $J_j := \{-m+1,\cdots,2^j-m\}$. Since the bases $\{B_{i,m,j}\}_{i\in I_j} \cup \{\psi_{j,i}\}_{i\in J_j}$ are linear independent, then $\{B_{i,m,j}\}_{i\in I_j} \cup \{\psi^N_{j,i}\}_{i\in J_j}$ consist a linear independent set. On the other hand, if $f \in V_{j+1}$, then by $V_{j+1} = V_j \oplus W_j$ there exist the constants $c_{j,i}$ and $d_{j,i}$ that f can be uniquely stated by

$$f(x) = \sum_{i\in I_j} c_{j,i}B_{i,m,j}(x) + \sum_{i\in J_j} d_{j,i}\psi_{j,i}(x). \tag{3.2}$$

Now, by (3.2) we have

$$\begin{aligned}
f(x) =& \sum_{i\in I_j\setminus\{-m+1,2^j-1\}} c_{j,i}B_{i,m,j}(x) + c_{j,-m+1}B_{-m+1,m,j}(x) + c_{j,2^j-1}B_{2^j-1,m,j}(x)\\
&+\sum_{i=-m+1}^{-1} d_{j,i}(\psi_{j,i}(x)-\alpha_{j,i}B_{-m+1,m,j}(x)) + \sum_{i=0}^{2^j-2m+1} d_{j,i}\psi_{j,i}(x)\\
&+\sum_{i=2^j-2m+2}^{2^j-m} d_{j,i}(\psi_{j,i}(x)-\beta_{j,i}B_{2^j-1,m,j}(x)) + \sum_{i=-m+1}^{-1} d_{j,i}\alpha_{j,i}B_{-m+1,m,j}(x)\\
&+\sum_{i=2^j-2m+2}^{2^j-m} d_{j,i}\beta_{j,i}B_{2^j-1,m,j}(x)\\
=& \sum_{i\in I_j\setminus\{-m+1,2^j-1\}} c_{j,i}B_{i,m,j}(x) + \Big(c_{j,-m+1}+\sum_{i=-m+1}^{-1} d_{j,i}\alpha_{j,i}\Big)B_{-m+1,m,j}(x)\\
&+\Big(c_{j,2^j-1}+\sum_{i=2^j-2m+2}^{2^j-m} d_{j,i}\beta_{j,i}\Big)B_{2^j-1,m,j}(x) + \sum_{i\in J_j} d_{j,i}\psi^N_{j,i}(x).
\end{aligned}$$

Then, f can be written as an unique combination of the basis functions in V_j and W_j^N, i.e.,

$$V_{j+1} = V_j \oplus W_j^N,$$

where $\oplus$ denotes a direct sum but not an orthogonal direct sum. $\square$

Fig. 1 shows some of these modified wavelet bases for $m=2$ at the scale $j=2$. By Lemmas 2.2 and 2.3, we have 2^j-2m+2 and $2(m-1)$ inner wavelets and boundary wavelets respectively. Then, as the level j increases, the number of inner wavelets would be many more than the boundary wavelets. Moreover, for $j\neq\tilde{j}$

$$\langle \psi^I_{j,i}, \psi^I_{\tilde{j},\tilde{i}}\rangle = 0, \quad i=0,\cdots,2^j-2m+1, \quad \tilde{i}=0,\cdots,2^{\tilde{j}}-2m+1,$$

where $\psi^I_{j,i}$ and $\psi^I_{\tilde{j},\tilde{i}}$ are inner wavelets. On the other hand, for $j<\tilde{j}$ we have

$$\langle \psi^L_{j,i}, \psi^I_{\tilde{j},\tilde{i}}\rangle = 0, \quad i=-m+1,\cdots,-1, \quad \tilde{i}=0,\cdots,2^{\tilde{j}}-2m+1$$

and

$$\langle \psi^R_{j,i}, \psi^I_{\tilde{j},\tilde{i}}\rangle = 0, \quad i=2^j-2m+2,\cdots,2^j-m, \quad \tilde{i}=0,\cdots,2^{\tilde{j}}-2m+1,$$

where $\psi^L_{j,i}$ and $\psi^R_{j,i}$ are the left and right boundary wavelets, respectively. Then, the coefficient matrix $A=(\langle\psi_{j,i},\psi_{\tilde{j},\tilde{i}}\rangle)$ in both cases of MKBSW and modified MKBSW would be sparse.

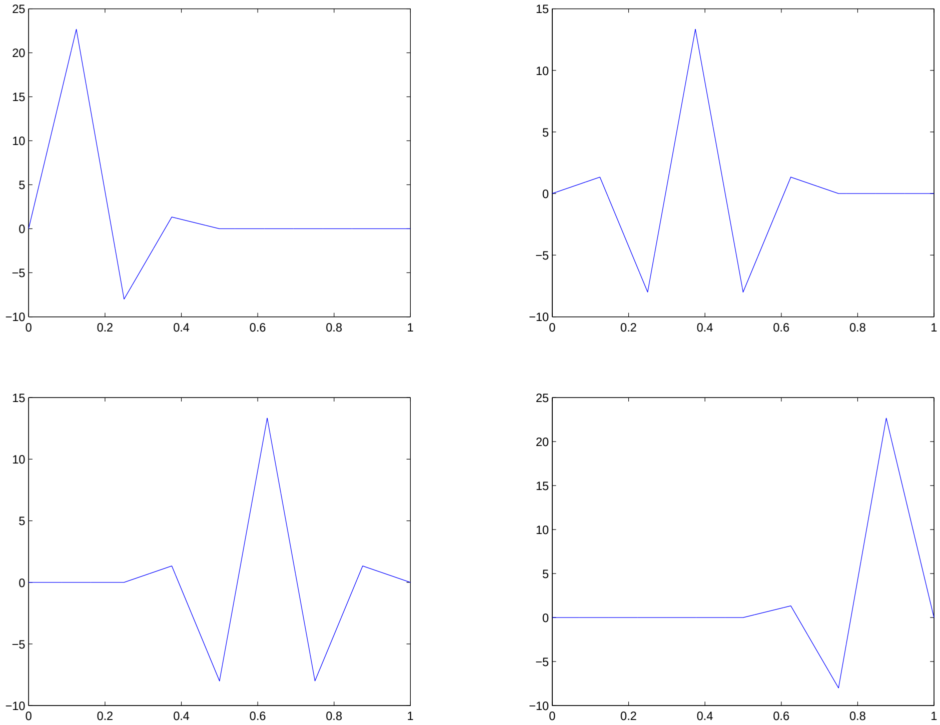

Figure 1: The wavelets $\psi^N_{2,i}$, $i=-1,0,1,2$.

3.2 Two dimensional B-spline wavelets

One can construct the two dimensional wavelet basis functions by tensor product of one dimensional wavelet bases. For this purposes, let B_j and Ψ_j are the set of scaling functions and wavelet bases, respectively so that

$$B_j := \{B_{i,m,j} : i = -m+1, \cdots, 2^j - 1\}, \tag{3.3a}$$
$$\Psi^N_j := \{\psi^N_{j,i} : i = -m+1, \cdots, 2^j - m\}. \tag{3.3b}$$

Also, we assume that $\{V^1_j, B^1_j\}$ and $\{V^2_j, B^2_j\}$ are two multi-resolution analysis (MRA) on the coordinates x and y with corresponding wavelets Ψ^{N1}_j and Ψ^{N2}_j, respectively, i.e.,

$$B^1_j = \{B_{-m+1,m,j}(x), \cdots, B_{2^j-1,m,j}(x)\}, \qquad B^2_j = \{B_{-m+1,m,j}(y), \cdots, B_{2^j-1,m,j}(y)\},$$
$$\Psi^{N1}_j = \{\psi^N_{j,-m+1}(x), \cdots, \psi^N_{j,2^j-m}(x)\}, \qquad \Psi^{N2}_j = \{\psi^N_{j,-m+1}(y), \cdots, \psi^N_{j,2^j-m}(y)\}.$$

Let us to define the space V^{2D}_j as

$$V^{2D}_j := V^1_j \otimes V^2_j. \tag{3.4}$$

Now, by (3.4) and distribution of tensor product over addition, we have

$$\begin{aligned} V_{j+1}^{2D} =& V_{j+1}^{1} \otimes V_{j+1}^{2} = (V_j^1 \oplus W_j^{N1}) \otimes (V_j^2 \oplus W_j^{N2}) \\ =& (V_j^1 \otimes V_j^2) \oplus (V_j^1 \otimes W_j^{N2}) \oplus (W_j^{N1} \otimes V_j^2) \oplus (W_j^{N1} \otimes W_j^{N2}). \end{aligned}$$

Therefore, four families of functions are generated in $L^2([0,1] \times [0,1])$ that contain a family of scaling functions and three families of wavelet functions $\mathbf{\Psi}_j^{N1}$, $\mathbf{\Psi}_j^{N2}$ and $\mathbf{\Psi}_j^{N3}$. The wavelet families are defined as follows:

$$\begin{aligned} \mathbf{B}_j &:= B_j^1 \otimes B_j^2 = \{B_{-m+1,m,j}(x), \cdots, B_{2^j-1,m,j}(x)\} \otimes \{B_{-m+1,m,j}(y), \cdots, B_{2^j-1,m,j}(y)\}, \\ \mathbf{\Psi}_j^{N1} &:= B_j^1 \otimes \Psi_j^{N2} = \{B_{-m+1,m,j}(x), \cdots, B_{2^j-1,m,j}(x)\} \otimes \{\psi_{j,-m+1}^N(y), \cdots, \psi_{j,2^j-m}^N(y)\}, \\ \mathbf{\Psi}_j^{N2} &:= \Psi_j^{N1} \otimes B_j^2 = \{\psi_{j,-m+1}(x), \cdots, \psi_{j,2^j-m}(x)\} \otimes \{B_{-m+1,m,j}(y), \cdots, B_{2^j-1,m,j}(y)\}, \\ \mathbf{\Psi}_j^{N3} &:= \Psi_j^{N1} \otimes \Psi_j^{N2} = \{\psi_{j,-m+1}^N(x), \cdots, \psi_{j,2^j-m}^N(x)\} \otimes \{\psi_{j,-m+1}^N(y), \cdots, \psi_{j,2^j-m}^N(y)\}. \end{aligned}$$

It is readily seen that

$$V_{j+1}^{2D} = V_j^{2D} \oplus W_j^{N2D},$$

where the wavelet space W_j^{N2D} is defined as

$$W_j^{N2D} := \langle \mathbf{\Psi}_j^{N1}, \mathbf{\Psi}_j^{N2}, \mathbf{\Psi}_j^{N3} \rangle$$

and $\oplus$ denotes a direct sum but not an orthogonal direct sum.

Remark 3.1. We note that for solving a Dirichlet boundary value problem, the following basis functions are removed in V_{j+1}^{2D}:

$$B_{-m+1,m,j}(x) \otimes B_j^2, \qquad B_{2^j-1,m,j}(x) \otimes B_j^2, \tag{3.5a}$$
$$B_j^1 \otimes B_{-m+1,m,j}(y), \qquad B_j^1 \otimes B_{2^j-1,m,j}(y), \tag{3.5b}$$
$$B_{-m+1,m,j}(x) \otimes \Psi_j^{N2}, \qquad B_{2^j-1,m,j}(x) \otimes \Psi_j^{N2}, \tag{3.5c}$$
$$\Psi_j^{N1} \otimes B_{-m+1,m,j}(y), \qquad \Psi_j^{N1} \otimes B_{2^j-1,m,j}(y). \tag{3.5d}$$

Fig. 2 shows a family of scaling functions and three families of the modified wavelet functions.

4 A method for solution of the system

Let Ω be unit square and consider the problem:

$$Lu = f, \qquad \text{in } \Omega, \tag{4.1a}$$
$$u = 0, \qquad \text{on } \partial\Omega, \tag{4.1b}$$

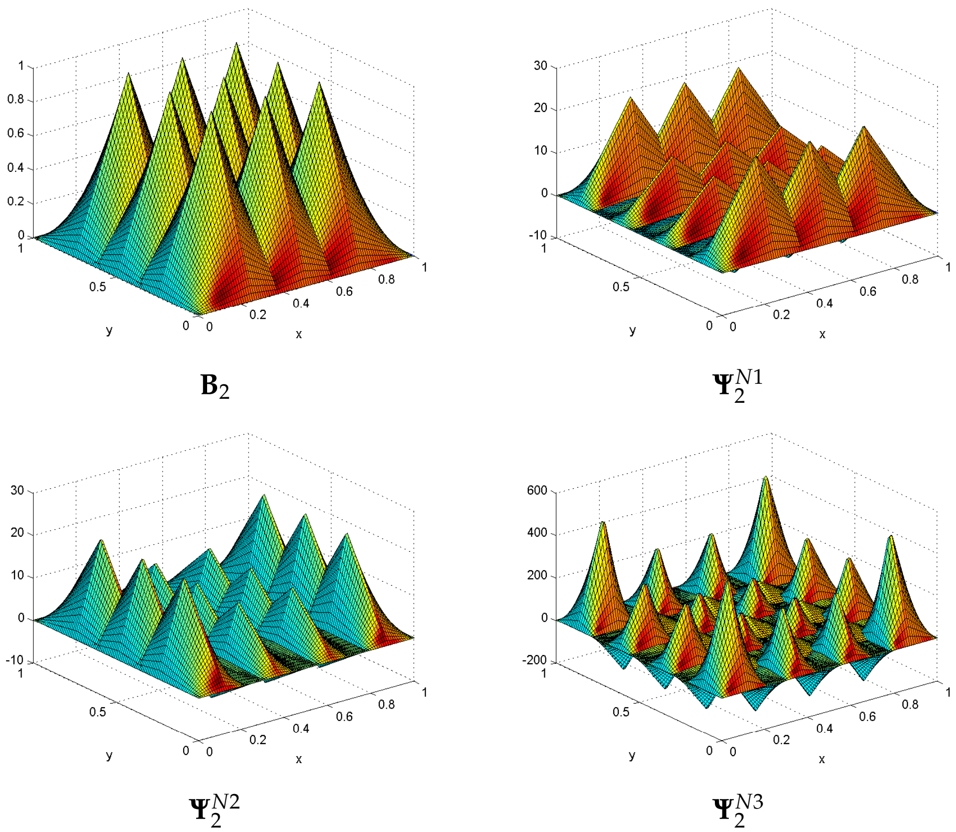

Figure 2: Scaling functions and three families of modified wavelet functions.

where

$$Lu = -\sum_{i,j} \frac{\partial}{\partial x_i} a_{i,j} \frac{\partial u}{\partial x_j} + au,$$

such that $a_{i,j}(x)$ is symmetric uniformly positive definite and $a(x) \geq 0$ in Ω. By the previous section, there is a sequence of nested finite-dimensional inner product spaces

$$V_{j_0}^{2D} \subset V_{j_0+1}^{2D} \subset \cdots \subset V_J^{2D},$$

where $j_0 \geq \lceil \log_2(2m-1) \rceil$. In addition, let $a(\cdot,\cdot)$ and $(\cdot,\cdot)_j$ be symmetric positive definite bilinear forms on V_j^{2D} for $j = j_0, \cdots, J$. The variational form of (4.1) in the finest level J is finding the solution of the following problem: Given $f \in V_J^{2D}$, find $u \in V_J^{2D}$ such that

$$a(u,v) = f(v), \quad \forall v \in V_J^{2D}. \tag{4.2}$$

By Lax-Milgram Theorem, the system

$$AU = F \tag{4.3}$$

produced by (4.2) has a unique solution (see [11]). By considering the Remark (3.1), it is readily seen that at level j, the dimension of matrix A is given by

$$dim(A) = (2^j + m - 3) \times (2^j + m - 3). \tag{4.4}$$

Hence, when the level j, increases, the dimension of A increases by multiplication of 2^{2j}. Then we should find a suitable method to solve the system (4.3). To this end, we need the following definition:

Definition 4.1. *Let $F = \{f_1, f_2, \cdots, f_m\}$ and $G = \{g_1, g_2, \cdots, g_n\}$, for $m, n \in \mathbb{N}$. Then we define $a(F, G)$ as*

$$a(F, G) = (a(f_i, g_j))_{i,j}$$

for $1 \le i \le m$ and $1 \le j \le n$.

The general form of the matrix A in the space

$$V_{J+1}^{2D} = V_{j_0}^{2D} \oplus \bigoplus_{j=j_0}^{J} W_j^{N2D}$$

is as follows:

$$A = \begin{bmatrix} \mathbf{BB}_{j_0} & \mathbf{B\Psi}_{j_0} & \cdots & \mathbf{B\Psi}_J \\ (\mathbf{B\Psi}_{j_0})^T & \mathbf{\Psi\Psi}_{j_0,j_0} & \cdots & \mathbf{\Psi\Psi}_{j_0,J} \\ \vdots & \vdots & \cdots & \vdots \\ (\mathbf{B\Psi}_J)^T & \mathbf{\Psi\Psi}_{J,j_0} & \cdots & \mathbf{\Psi\Psi}_{J,J} \end{bmatrix}, \tag{4.5}$$

where

$$\begin{aligned} \mathbf{BB}_{j_0} &:= a(\mathbf{B}_{j_0}, \mathbf{B}_{j_0}), \\ \mathbf{B\Psi}_k &:= [a(\mathbf{B}_{j_0}, \mathbf{\Psi}_k^{N1}) \quad a(\mathbf{B}_{j_0}, \mathbf{\Psi}_k^{N2}) \quad a(\mathbf{B}_{j_0}, \mathbf{\Psi}_k^{N3})], \\ \mathbf{\Psi\Psi}_{k,h} &:= \begin{bmatrix} a(\mathbf{\Psi}_k^{N1}, \mathbf{\Psi}_h^{N1}) & a(\mathbf{\Psi}_k^{N1}, \mathbf{\Psi}_h^{N2}) & a(\mathbf{\Psi}_k^{N1}, \mathbf{\Psi}_h^{N3}) \\ a(\mathbf{\Psi}_k^{N2}, \mathbf{\Psi}_h^{N1}) & a(\mathbf{\Psi}_k^{N2}, \mathbf{\Psi}_h^{N2}) & a(\mathbf{\Psi}_k^{N2}, \mathbf{\Psi}_h^{N3}) \\ a(\mathbf{\Psi}_k^{N3}, \mathbf{\Psi}_h^{N1}) & a(\mathbf{\Psi}_k^{N3}, \mathbf{\Psi}_h^{N2}) & a(\mathbf{\Psi}_k^{N3}, \mathbf{\Psi}_h^{N3}) \end{bmatrix} \end{aligned}$$

for $k, h \in \{j_0, j_0 + 1, \cdots, J\}$.

A schematic representation of the matrix A for $m = 2$, $j_0 = 2$ and $J = 3$ is seen in Fig. 3 and the block matrix A can be considered as

$$A = \begin{bmatrix} A_1 & A_2 \\ A_2^T & A_3 \end{bmatrix},$$

where

$$A_1 = \begin{bmatrix} \mathbf{BB}_2 & \mathbf{B\Psi}_2 \\ (\mathbf{B\Psi}_2)^T & \mathbf{\Psi\Psi}_{2,2} \end{bmatrix}, \quad A_2 = \begin{bmatrix} \mathbf{B\Psi}_3 \\ \mathbf{\Psi\Psi}_{2,3} \end{bmatrix}, \quad A_3 = \begin{bmatrix} \mathbf{\Psi\Psi}_{3,3} \end{bmatrix}.$$

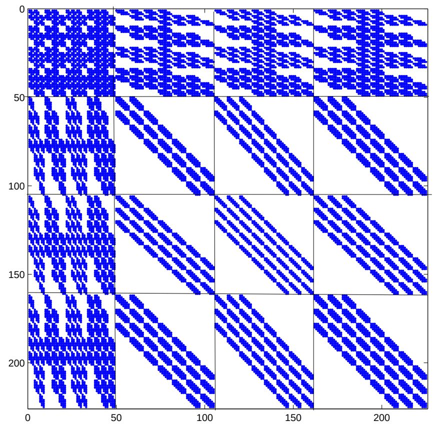

Figure 3: A schematic representation of the matrix A.

Since the matrix A is symmetric positive definite, it can be factorized by $A = LDL^T$ where

$$L = \begin{bmatrix} I & 0 \\ A_2^T A_1^{-1} & I \end{bmatrix}, \quad D = \begin{bmatrix} A_1 & 0 \\ 0 & A_3 - A_2^T A_1^{-1} A_2 \end{bmatrix}.$$

Hence, the system (4.3) can be replaced by

$$LDL^T U = F,$$

that is solved as

$$U = (L^T)^{-1} D^{-1} L^{-1} F = \begin{bmatrix} I & -A_1^{-1} A_2 \\ 0 & I \end{bmatrix} \begin{bmatrix} A^{-1} & 0 \\ 0 & H \end{bmatrix} \begin{bmatrix} I & 0 \\ -A_2^T A_1^{-1} & I \end{bmatrix} F,$$

where $H = (A_3 - A_2^T A_1^{-1} A_2)^{-1}$. This factorization is also generalizable for higher dimensional case. For

$$A = \begin{bmatrix} A_1 & A_2 & A_3 \\ A_2^T & A_4 & A_5 \\ A_3^T & 1A_5^T & A_6 \end{bmatrix},$$

the factorization LDL^T is defined by

$$L = \begin{bmatrix} I & 0 & 0 \\ A_2^T A_1^{-1} & I & 0 \\ A_3^T A_1^{-1} & (A_5^T - A_3^T A_1^{-1} A_2)(A_4 - A_2^T A_1^{-1} A_2)^{-1} & I \end{bmatrix},$$

$$D = \begin{bmatrix} A_1 & 0 & 0 \\ 0 & A_4 - A_2^T A_1^{-1} A_2 & 0 \\ 0 & 0 & K \end{bmatrix},$$

where A_1 is a square matrix and

$$K = A_6 - A_3^T A_1^{-1} A_3 - (A_5^T - A_3^T A_1^{-1} A_2)(A_4 - A_2^T A_1^{-1} A_2)^{-1}(A_5 - A_2^T A_1^{-1} A_3).$$

5 Saint-Venant equation

Unsteady flow is of great interest to hydraulic engineers. Such flows can be described by the Saint-Venant equations which consist of the conservation of mass and momentum equations. The Saint-Venant equations also are nonlinear hyperbolic partial differential equations. However, a general closed-form solution of these equations is not available, except for certain special simplified conditions and they must be solved using an appropriate numerical technique [6]. In typical hydraulic textbooks (e.g., see [2] and [8]) these equations are derived from the incompressible Navier-Stokes equations. Over the past few years, a wide range of numerical schemes from the finite difference [3], finite element (see [13] and [15]) and finite volume [4] methods that have been applied to the open channel flow equations.

In this section, we present a solution to solve the Saint-Venant equations by the modified multiple knot B-spline wavelets that given in Section 3. To do this, we consider the initial-boundary value Saint-Venant problem for unsteady flow in an open channel having no lateral inflow or outflow for one dimensional as:

$$\begin{cases} \dfrac{\partial Q}{\partial t} + \dfrac{\partial}{\partial x}\Big(\dfrac{Q^2}{A}\Big) + gA\dfrac{\partial h}{\partial x} + \dfrac{gn^2|Q|Q}{R^{4/3}A} = 0, & \text{momentum equation}, \\ \dfrac{\partial h}{\partial t} + \dfrac{1}{B}\dfrac{\partial Q}{\partial x} = 0, & \text{continuity equation}, \\ Q(x,0) = Q^0, & 0 \le x < L, \\ h(x,0) = h^0, & 0 \le x \le L, \\ Q(L,t) = 0, & t \ge 0, \\ h(0,t) = h_0, & t > 0, \end{cases} \tag{5.1}$$

in which x = distance along the channel length, t = time, A = flow area, B = top water surface width, g = acceleration due to gravity, Q = discharge, h = water surface elevation, R = hydraulic radius, n = Manning coefficient, and L = length of channel, also h^0, h_0 and Q^0 are positive constant scalers. In general A and R are the functions of h (i.e., $A = A(h)$, $R = R(h)$).

Now, we are ready to explain the discretization process for the Saint-Venant equation 5.1.

5.1 Discretization of Saint-Venant equations

In order to present the variational form of Saint-Venant equations, we focus our attention on the discretization with respect to the time variable. Thus, we choose a positive integer N, let Δt denote the corresponding time-step: $\Delta t = T/N$ and t_n the subdivisions of $[0,T]$:

$$t_n = n\Delta t, \quad 0 \le n \le N.$$

For linearity, we consider the terms of Saint-Venant equations as follows:

$$\begin{cases} \dfrac{\partial Q(x,t_n)}{\partial t} + \dfrac{\partial}{\partial x}\Big(\dfrac{Q^2(x,t_{n+1})}{A(x,t_n)}\Big) + gA(x,t_n)\dfrac{\partial h(x,t_{n+1})}{\partial x} + \dfrac{gn^2|Q(x,t_n)|Q(x,t_{n+1})}{R^{4/3}(x,t_n)A(x,t_n)} = 0, \\ \dfrac{\partial h(x,t_n)}{\partial t} + \dfrac{1}{B}\dfrac{\partial Q(x,t_{n+1})}{\partial x} = 0. \end{cases} \tag{5.2}$$

Now, by Taylor expansion we get

$$\begin{cases} (a) \ \dfrac{\partial Q(x,t_n)}{\partial t} \cong \dfrac{Q(x,t_{n+1}) - Q(x,t_n)}{\Delta t}, \\ (b) \ \dfrac{\partial h(x,t_n)}{\partial t} \cong \dfrac{h(x,t_{n+1}) - h(x,t_n)}{\Delta t}. \end{cases} \tag{5.3}$$

Moreover

$$\begin{aligned} Q^2(x,t_{n+1}) &\cong Q^2(x,t_n) + \Delta t \frac{\partial Q^2(x,t_n)}{\partial t} \\ &\cong Q^2(x,t_n) + 2\Delta t Q(x,t_n)\frac{\partial Q(x,t_n)}{\partial t}. \end{aligned} \tag{5.4}$$

Then, by substituting Eq. (5.3a) in Eq. (5.4) we have

$$Q^2(x,t_{n+1}) \cong -Q^2(x,t_n) + 2Q(x,t_n)Q(x,t_{n+1}). \tag{5.5}$$

Substituting Eqs. (5.3) and (5.5) into Eq. (5.2) and simplifying, we can write the discrete form of (5.1) as follows:

$$\begin{cases} \dfrac{1}{\Delta t}Q(x,t_{n+1}) + \dfrac{\partial}{\partial x}\Big(\dfrac{2Q(x,t_n)Q(x,t_{n+1})}{A(x,t_n)}\Big) + gA(x,t_n)\dfrac{\partial h(x,t_{n+1})}{\partial x} & \\ + \dfrac{gn^2|Q(x,t_n)|Q(x,t_{n+1})}{R^{4/3}(x,t_n)A(x,t_n)} = \dfrac{1}{\Delta t}Q(x,t_n) + \dfrac{\partial}{\partial x}\Big(\dfrac{Q^2(x,t_n)}{A(x,t_n)}\Big), & \\ \dfrac{1}{\Delta t}h(x,t_{n+1}) + \dfrac{1}{B}\dfrac{\partial Q(x,t_{n+1})}{\partial x} = \dfrac{1}{\Delta t}h(x,t_n), & \\ Q(x,0) = Q^0, & 0 \le x < L, \\ h(x,0) = h^0, & 0 \le x \le L, \\ Q(L,t_n) = 0, & n = 0,\cdots,N, \\ h(0,t_n) = h_0, & n = 1,\cdots,N. \end{cases} \tag{5.6}$$

5.2 Variational weak form

In order to consist the variational form of problem (5.6), we first note that the value of h is nonzero in the first of channel (i.e., the constant h_0), then we can consider

$$H(x,t_{n+1}):=h(x,t_{n+1})-h_0.$$

Now, the variational form of problem (5.6) is that find $Q(x,t_{n+1})\in V=\{Q(x,t_k)\in H^1(\Omega):Q(L,t_k)=0,\ \ k=0,\cdots,N\}$, and $H(x,t_{n+1})\in S=\{H(x,t_k)\in H^1(\Omega):H(0,t_k)=0,\ \ k=1,\cdots,N\}$ such that

$$d(H,v)+m(Q,v)+b(Q,v)=(\alpha,v)_0,\qquad \forall v\in S, \tag{5.7a}$$
$$s(H,e)+w(Q,e)=(\beta,e)_0,\qquad \forall e\in V, \tag{5.7b}$$

which $\Omega=[0,L]$, $(\cdot,\cdot)_0$ is an inner product in the $L_2(\Omega)$ space, and the bilinear forms on $V\times S$ are given respectively by

$$m(Q,v)=\int_\Omega\Big(\frac{1}{\Delta t}+\frac{gn^2|Q(x,t_n)|}{R^{4/3}(x,t_n)A(x,t_n)}\Big)Q(x,t_{n+1})vdx, \tag{5.8a}$$
$$b(Q,v)=-2\int_\Omega\frac{Q(x,t_n)}{A(x,t_n)}Q(x,t_{n+1})v'dx+\frac{2Q(x,t_n)Q(x,t_{n+1})}{A(x,t_n)}v|_{\partial\Omega}, \tag{5.8b}$$
$$d(H,v)=-g\int_\Omega H(x,t_{n+1})(A(x,t_n)v)'dx+gA(x,t_n)H(x,t_{n+1})v|_{\partial\Omega}, \tag{5.8c}$$
$$s(H,e)=\frac{1}{\Delta t}\int_\Omega H(x,t_{n+1})edx, \tag{5.8d}$$
$$w(Q,e)=\frac{-1}{B}\int_\Omega Q(x,t_{n+1})e'dx+\frac{1}{B}Q(x,t_{n+1})e|_{\partial\Omega}, \tag{5.8e}$$
$$(\alpha,v)=\int_\Omega \alpha vdx, \tag{5.8f}$$

where $\partial\Omega$ is the boundary of Ω and $v|_{\partial\Omega}$ the restriction of v on $\partial\Omega$.

Remark 5.1. Solving the Saint-Venant equations by numerical schemes like finite difference and finite element methods lead to some non-favorite oscillations for water surface elevation. The reason for these oscillations lies in the method of approximation for the non-linear terms. One of the ways to smooth these oscillations is adding artificial viscosity to the scheme [6]. Also, Average Rule is another method to eliminate oscillations. One can apply the average of nonlinear terms in space to eliminate oscillations [14] or the average of $H(x,t_n)$ and $Q(x,t_n)$ in space for time $t=t_{n+1}$ for finite element method [17, 19]. Since using the above heuristic techniques may ruin the stability, we did not use them and apply multiple knot B-spline wavelet directly.

6 Numerical results

In this section, we give some examples. All examples are coded by MATLAB software. The first two examples are considered for Poisson's problem

$$\begin{cases} -\Delta u = f, & \text{in } \Omega = [0,1] \times [0,1], \\ u = 0, & \text{on } \partial\Omega, \end{cases} \tag{6.1}$$

which f is defined such that the exact solution is

$$u = x(1-x)y(1-y).$$

We solve Problem (6.1) by Galerkin and Petrov-Galerkin's methods.

Example 6.1. In the first example, we show the solution (6.1) by Galerkin's method at level $J = 3$ with $m = 2$ and $j_0 = 2$. The variational form of (6.1) is that: find

$$u^h \in V_{j_0}^{2D} \oplus \bigoplus_{j=j_0}^{J} W_j^{N2D}$$

such that

$$a(u^h, v^h) = f(v^h), \quad \forall v^h \in V_{j_0}^{2D} \oplus \bigoplus_{j=j_0}^{J} W_j^{N2D}. \tag{6.2}$$

Figs. 4 and 5 show the exact and approximated solutions at level 3, respectively. As is seen, the approximated solution is in good agreement with the exact solution. We define the relative error by

$$\delta(\mathbf{u^h}) = \frac{\|\mathbf{u} - \mathbf{u^h}\|_{\ell_2}}{\|\mathbf{u}\|_{\ell_2}},$$

where $\mathbf{u} = (u(x_p, y_q))_{p,q}$ and $\mathbf{u}^h = (u^h(x_p, y_q))_{p,q}$ for $x_p = p\Delta x, p = 0, 1, \cdots, 100$ and $x_q = q\Delta y$, $q = 0, 1, \cdots, 100$ with $\Delta x = \Delta y = 1/100$. We show the relative error in Fig. 6. As we observe, the error decreases when the level increases. In addition, we present a comparison between the relative error of MKBSW and that of finite element method. To solve the Poisson's problem 6.1 by finite element method, we develop the sequence grid in a standard way. To define the coarse grid, we start by breaking the unit square into four smaller squares of side length 1/2 and then dividing each smaller square into two triangles by connecting the lower left hand corner. Subsequently, finer grids are developed as in the introduction, i.e., by dividing each triangle into the four triangles formed by the edges of the original triangle and the lines connecting the centers of theses edges. The space V_j for finite element method is defined to be the set of continuous functions on Ω which are piecewise linear on the 2^jth triangulation and vanish on $\partial\Omega$.

The relative error of both MKBSW and FEM is given in Table 1. As we expect, when the level increases, the relative error of MKBSW decreases significantly and moreover, the relative error of MKBSW is less than that of the finite element method (FEM).

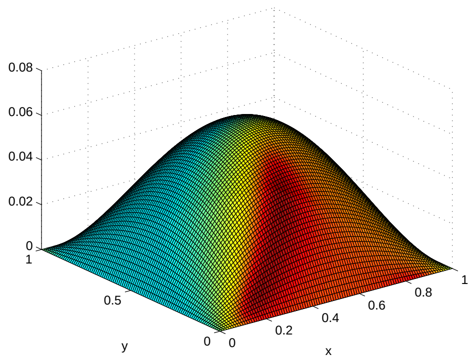

Figure 4: The exact solution.

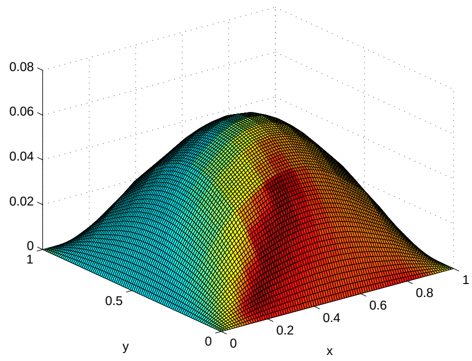

Figure 5: The approximated solution at $J=3$.

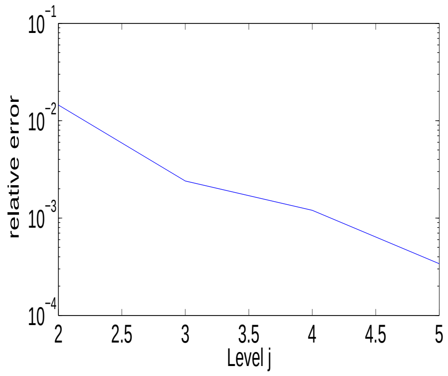

Figure 6: The relative error in $J=2,3,4,5$.

Table 1: The relative error of MKBSW and FEM for Poisson's problem.

Method	$j:=2$	$j:=3$	$j:=4$	$j:=5$
MKBSW	0.0158	0.0041	0.0010	0.0006
FEM	0.0892	0.0488	0.0127	0.0073

Example 6.2. In the second example, we show the solution (6.1) by Petrov-Galerkin's method at level $J=3$ with $m=2$ and $j_0=2$. The variational form of (6.1) is that: find

$$u^h \in V_{j_0}^{2D} \oplus \bigoplus_{j=j_0}^{J} W_j^{N2D}$$

such that

$$a(u^h, v^h) = f(v^h), \quad \forall v^h \in V_{j_0}^{2D} \oplus \bigoplus_{j=j_0}^{J} W_j^{2D}. \tag{6.3}$$

Fig. 7 show the approximated solution at level 3. We observe that like Example 6.1, this approximated solution is in a good agreement with exact solution, however the Galerkin's method approximates better than the Petrov-Galerkin's method for Problem 6.1.

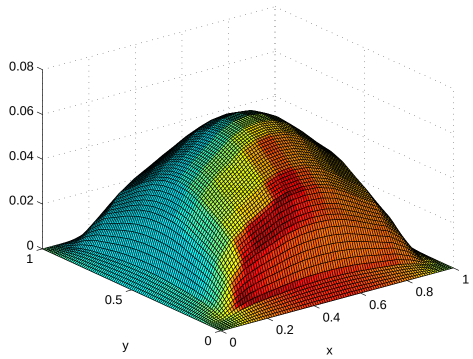

Figure 7: The approximated solution at $J = 3$.

Now, we solve the Saint-Venant equations for a rectangular channel.

Example 6.3. The task of estimating the movement of a surge (or shock) or a dam-break wave, resulting from the sudden up-stream opening (or the sudden downstream closure) of a sluice gate for emergencies or dam failures, has occupied the attention of researchers as well as practicing engineers for several decades. The determination of the surge height at different locations along the channel provides important information for the design of the bank height. The dreadful disaster due to the dam-break flood wave reminds the decision-makers to pay more attention to the dam-safety problem. We consider an open channel with rectangular cross section that its bottom width is 6.1m. The bottom slope is 0.00008, Manning coefficient $n = 0.013$ and the length of channel is 20m. The initial conditions in the channel are 5.79m-depth and a steady discharge of 126m^3/s. The water surface level in reservoir is constant at the up-stream end and also the sluice gate at the downstream end of the channel is suddenly closed at time $t = 0$. We also solved this problem by finite difference and finite element methods. Fig. 8 shows the flow depth in the channel at time $t = 0.5$s by finite element, finite difference and multiple knot B-spline wavelet methods. As we see, theses methods are

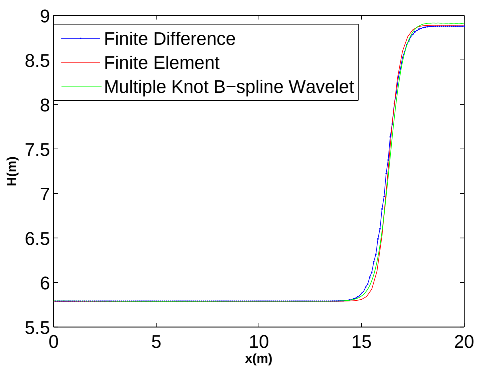

Figure 8: Flow depth in the rectangular channel at time $t = 0.5$s obtained by finite element, finite difference and multiple knot B-spline wavelet methods.

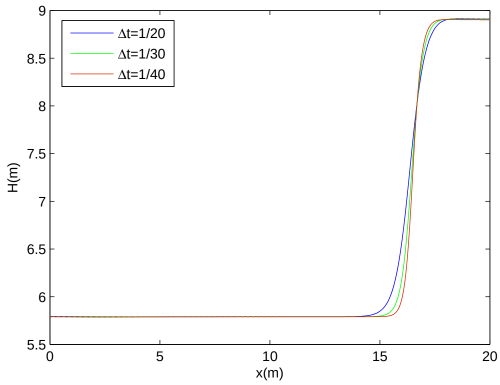

Figure 9: Flow depth at several Δt values for $m = 3$, $j_0 = 2$ and $J = 3$ at time $t = 0.5$s.

in good agreements.

Fig. 9 also shows the flow depth in several Δt for $m = 3$, $j_0 = 2$ and $J = 3$ at time $t = 0.5$s.

Example 6.4. We consider an open rectangular channel having a bottom width of 6.1m is carrying a flow of 126m^3/s. The bottom slope is 0.04, Manning coefficient $n = 0.00008$ and the channel length is 20m. We consider flow depth $h^0 = 6.5949$m. Suppose that a sluice gate at the downstream end is suddenly closed at time $t = 0$. We solved this problem by multiple knot B-spline wavelet and finite element methods. Fig. 10 shows the flow depth in the channel at time $t = 0.3$s.

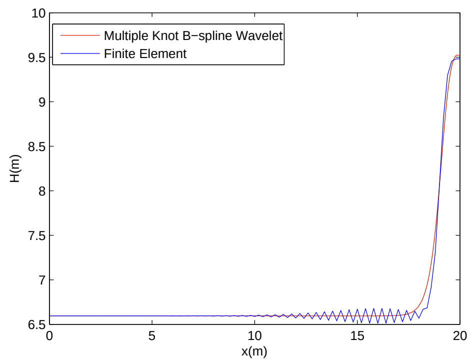

Figure 10: Flow depth in the rectangular channel at time $t = 0.3$s by multiple knot B-spline wavelet method with $m = 3$, $J = 3$ and finite element method (without the averaging rule).

7 Conclusions

We have studied the construction of semi-orthogonal multiple knot B-spline wavelets.Then, we have modified these wavelets for solving the elliptic partial differential equations with (partially) Dirichlet boundary conditions. Moreover, a discussion on the solution of discretized system by Galerkin and Petrov-Galerkin methods has been presented. Also, the hyperbolic equation of Saint-Venant has been solved by multiple knot B-spline wavelets and the efficiency of this method has been compared with finite element and finite difference methods.

References

[1] N. AGHAZADEH AND H. MESGARANI, *Solving non-linear fredholm integro-differential equation*, World Appl. Sci. J., 7 (2009), pp. 50–56.

[2] A. O. AKAN, Open Channel Hydraulics, Elsevier, Oxford UK, 2006.

[3] M. AMEIN AND H. L. CHU, *Implicit numerical modeling of unsteady flows*, ASCE J. Hydr. Eng., 101 (1974), pp. 717–731.

[4] E. AUDUSSE AND M. O. BRISTEAU, *Finite-volume solvers for a multilayer Saint-Venant system*, Int. J. Appl. Math. Comput. Sci., 17(3) (2007), pp. 311–320.

[5] K. BITTNER, *Biorthogonal spline wavelets on the interval*, in Wavelets and splines: Athens 2005, Mod. Methods Math., pp. 93–104, Nashboro press, Brentwood, TN, 2006.

[6] M. H. CHAUDHRY, Open-Channel Flow, 2nd ed., Springer, 2008.

[7] X. CHEN, J. XIANG, B. LI AND Z. HE, *A study of multiscale wavelet-based elements for adaptive finite element analysis*, Adv. Eng. Soft., 41 (2010), pp. 196–205.

[8] V. T. CHOW, Open Channel Hydraulics, McGraw-Hill, New York, 1959.

[9] C. K. CHUI AND E. QUAK, *Wavelet on a bounded interval*, in: D. Braess and L. L. Schumaker, editors, Numerical Methods Of Approximation Theory, Basel: Birkhauser Verlag; (1992), pp. 57–76.

[10] C. K. CHUI AND J. Z. WANG, *A cardinal spline approach to wavelets*, Proc. Amer. Math. Soc., 113 (1991), pp. 785–793.

[11] P. G. CIARLET, The Finite Element Methods for Elliptic Problems, North Holland, Amesterdam, (1978).

[12] I. DAUBECHIES, *Orthonormal bases of compactly supported wavelets*, Commun. Pure Appl. Math., 41 (1988), pp. 909–996.

[13] F. E. HICKS, Finite Element Modeling of Open Channel Flow, University of Alberta, Ph.D thesis, 1990.

[14] J. GRANATOWICZ AND R. SZYMKIEWICZ, *Comparison of efficency of the solution of the Saint-Venant equations by finite element method and finite difference method*, Arch. Hydr., 3-4 (1989), pp. 199–210.

[15] R. SZYMKIEWICZ, *Finite element method for the solution of the Saint-Venant equation in the open channel network*, J. Hydr., 122 (1991), pp. 275–287.

[16] A. TAVAKOLI AND S. JAFARI, *New preconditioners for elliptic boundary value problems in multi-resolution space*, Sci. Bull., Series A. Appl. Math. Phys., to appear.

[17] A. TAVAKOLI AND F. ZARMEHI, *Adaptive finite element methods for solving Saint-Venant equations*, Scientia Iranica, Transactions B: Mech. Eng., 18 (2011), pp. 1321–1326.

[18] K. URBAN, *Wavelet Methods for Elliptic Partial Differential Equation*, G. H. Golub, A. M. Stuart and E. Suli, editors, University of Ulm, 2009.

[19] F. ZARMEHI, A. TAVAKOLI AND M. RAHIMPOUR, *On numerical stabilization in the solution of Saint-Venant equations using finite element method* Comput. Math. Appl., 62 (2011), pp. 1957–1968.